ACS OMEGA

http://pubs.acs.org/journal/acsodf

Article

Surprises in the Solvent-Induced Self-Ionization in the Uranium Tetrahalide UX_4 (X = Cl, Br, I)/Ethyl Acetate System

H. Lars Deubner, Tim Graubner, Magnus R. Buchner, Florian Weigend, Sergei I. Ivlev, Antti J. Karttunen, and Florian Kraus*

Cite This: *ACS Omega* 2022, 7, 11995−12003

Read Online

ACCESS | Metrics & More | Article Recommendations | Supporting Information

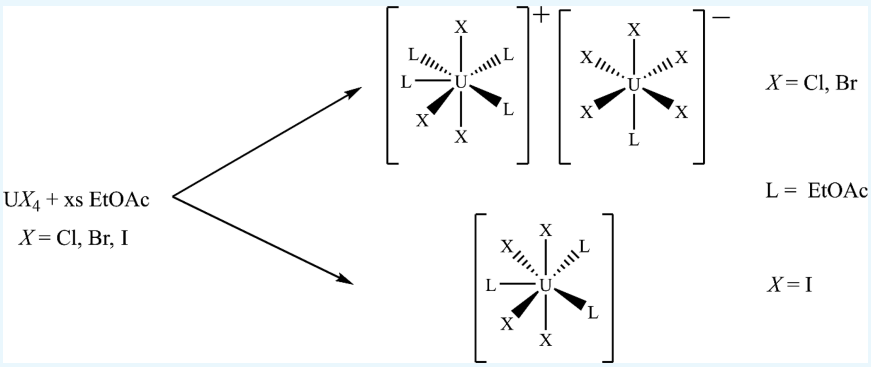

ABSTRACT: The reaction of the uranium(IV) halides UCl_4, UBr_4, or UI_4 with ethyl acetate (EtOAc) leads to the formation of the complexes $[UX_3(EtOAc)_4][UX_5(EtOAc)]$ (X = Cl, Br) or $[UI_4(EtOAc)_3]$. Thus, both UCl_4 and UBr_4 show self-ionization in ethyl acetate to a distorted pentagonal bipyramidal $[UX_3(EtOAc)_4]^+$ cation and a distorted octahedral $[UX_5(EtOAc)]^-$ anion. Surprisingly, the chloride and bromide compounds are not isotypic. While $[UCl_3(EtOAc)_4][UCl_5(EtOAc)]$ crystallizes in the orthorhombic crystal system, space group $P2_12_12_1$ at 250 K, the bromide compound crystallizes in the monoclinic crystal system, $P12_1/n1$ at 100 K. Unexpectedly, UI_4 does not show self-ionization but forms $[UI_4(EtOAc)_3]$ molecules, which crystallize in the monoclinic crystal system, $P2_1/c$, at 100 K. The compounds were characterized by single-crystal X-ray diffraction, IR, Raman, and NMR spectroscopy, as well as molecular quantum chemical calculations using solvent models.

INTRODUCTION

Self-ionization is a long known property of many inorganic compounds and has been proven to occur in the gas, liquid, and solid phases.[1−6] Water is certainly the best investigated example of a compound showing self-ionization. Neutral water contains only small concentrations of H_3O^+ and OH^- ions under ambient conditions, that is, the autoprotolysis constant is quite small. Other compounds that show self-ionization are liquid NH_3, BrF_3, anhydrous HF, and other amphoteric molecules.[3,7−10] Cl_2O_6 and N_2O_5 show electrically neutral molecular structures in the gas phase, but in the solid-state ionic structures, $[ClO_2]^+[ClO_4]^-$ and $[NO_2]^+[NO_3]^-$ are present.[11,12] In the solid state of PCl_5, tetrahedral $[PCl_4]^+$ cations and octahedral $[PCl_6]^-$ anions occur.[13−17] Self-ionization can also be induced by ligands, and the compounds $[TiF_2([15]crown-5)][Ti_4F_{18}]$, $[AuCl_2py_2][AuCl_4]\cdot 2$-$[AuCl_3py]$, $[NbF_4(Me_2S)_4][NbF_6]$, and $[(L^{Dipp})_2SbF_2][SbF_4]$ or $[Ta(N_3)_4(1,10\text{-phen})_2][M(N_3)_6]$, $[Be_2I_2(dmf)_4][Be_2I_6]$, and $[BePh(12\text{-crown-}4)][BePh_3]$ serve as examples.[18−29]

To the best of our knowledge, the first actinide complex resulting from self-ionization was reported in 1973.[30] The authors interpreted the UV−vis spectrum of the compound "$UCl_4(Me_2SO)_3$" and deduced its composition as $[UCl_2(Me_2SO)_6][UCl_6]$. This was confirmed by its crystal structure in 1975.[30,31] Only a couple of other U-containing compounds which show self-ionization were reported.[31−39] In most of them, an octahedral $[UX_6]^{2-}$ (X = Cl, Br, I) anion is present besides various cations. Examples are $[UCl_2(Me_2SO)_6][UCl_6]$, $[UBr_2(1H\text{-indene})(MeCN)_4]$-$[UBr_6]$, or the mixed-valent compound $[U(MeCN)_9][UI_6]$-I.[30,31,34,37] A few compounds are known containing an anion of the form $[UX_5L]^-$ (X = Cl, Br, I; L = organic ligand). Examples are $[UCl_3((EtC(O)N(Et)_2))_4]$, $[UCl_5(EtC(O)N$-$(Et)_2)]$, or $[Et_2OH][UX_5(Et_2O)]\cdot Et_2O$ (X = Br, I).[33,40,41]

While the chemistry of $[UO_2]^{2+}$-containing compounds in ethyl acetate is well examined,[42−50] surprisingly few ethyl

Received: January 10, 2022
Accepted: January 28, 2022
Published: April 1, 2022

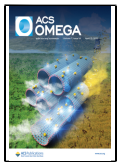

acetate containing complexes of U(IV) seem to be known. Herein we describe the reaction of the uranium(IV) halides UX_4 (X = Cl, Br, I) with ethyl acetate.

RESULTS AND DISCUSSION

The reaction of uranium(IV) chloride or bromide leads to the formation of complexes resulting from self-ionization of $[UX_3(EtOAc)_4][UX_5(EtOAc)]$ (X = Cl, Br), while the iodide does—surprisingly—not dissociate and is obtained as $[UI_4(EtOAc)_3]$. Scheme 1 gives an overview of the reaction conditions and products.

Scheme 1. Overview of the Reactions of the Uranium Halides UX_4 (X = Ck, Br, I) with EtOAc and the Respective Reaction Conditions

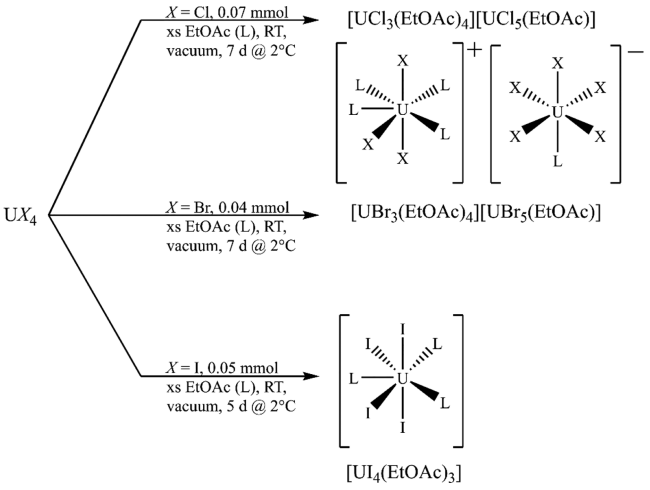

The starting materials were dissolved in an excess of EtOAc at room temperature. Then, a vacuum was applied to remove the solvent until crystallization started. These solutions were subsequently stored at 2 °C for a couple of days to allow for the growth of single crystals, which were filtered off. Details are available from the Experimental Section.

Crystal Structure of the Chloride. The blueish black compound $[UCl_3(EtOAc)_4][UCl_5(EtOAc)]$ crystallizes in the space group $P2_12_12_1$, No. 19, with a = 15.1255(4), b = 15.4634(7), c = 17.4324(7) Å, V = 4077.3(3) Å^3, and Z = 4 at T = 250 K. Unfortunately, the crystals broke apart upon cooling to 100 K, so the single-crystal X-ray structure determination had to be conducted at 250 K to prevent the shattering of the crystals. See Table 1 for selected crystallographic data and details of the structure determinations.

The uranium atom of the $[UCl_3(EtOAc)_4]^+$ cation is coordinated by seven ligands, three chloride atoms, and four ethyl acetate molecules, in the shape of a pentagonal bipyramid considering only the ligating atoms. The coordination polyhedron of the $[UCl_5(EtOAc)]^-$ anion is a slightly distorted octahedron where the central uranium atom is coordinated by five chlorido ligands and one ethyl acetate molecule. See Figure 1 for an impression.

The bond lengths between the uranium atom and the chlorido ligands in the cation range from 2.566(3) to 2.624(2) Å and from 2.556(4) to 2.588(3) Å in the anion. These distances are in good agreement with the literature.[32,35] The atomic distances between the uranium atom and the coordinating oxygen atoms of the ethyl acetate ligands range from 2.346(8) to 2.374(9) Å in the cation. For the disordered EtOAc ligands of the anion, the distances are 2.30(2) and 2.36(2) Å. The U−O distances are in agreement with the literature.[51−54] The C−H···Cl hydrogen bonds between ethyl acetate molecules and the chlorido ligands are comparable with those in compounds such as $[UCl_3(N,N\text{-diethylpropionamide})_4][UCl_5(N,N\text{-diethylpropionamide})]$.[33] Selected L−U−L (L = coordinating ligand atom) angles in the $[UCl_5(EtOAc)]^-$ anion range from ca. 81 to 98° and show a significant distortion of the octahedron-like coordination polyhedron, as expected. The pentagonal bipyramidal $[UCl_3(EtOAc)_4]^+$ cation is only slightly distorted with L−U−L angles between 69.4(3) and 74.6(2)° (ideal 72°) for the equatorial and between 88.8(2) and 91.51(11)° (ideal 90°) for the axial ligands. All distances and angles are however additionally biased as the compound shows a distinct disorder of the coordinated ethyl acetate molecule in the $[UCl_5(EtOAc)]^-$ anion. The closest U···U distance is between neighboring cations and anions with ca. 7.59 Å. The cations are surrounded by six anions in the shape of very distorted octahedra and vice versa with the U···U distances in a range from ca. 7.59 to 9.98 Å. However, the distortion is so severe that we could not identify any reasonable packing of cations and/or anions, such as in the NaCl structure type for example.

Crystal Structure of the Bromide. The reaction of uranium(IV) bromide with ethyl acetate leads to the formation of dark green $[UBr_3(EtOAc)_4][UBr_5(EtOAc)]$. Although the compound has a similar composition and the same structural constitution as the chloride described above, it is not isotypic. It crystallizes in the monoclinic crystal system, space group $P12_1/n1$, No. 14, with a = 15.7380(10), b = 17.5732(9), c = 16.2532(11) Å, V = 4111.2(5) Å^3, and Z = 4 at T = 100 K (Table 1). The uranium atom of the cation is again coordinated by seven ligands, three bromide atoms, and four ethyl acetate molecules, in the shape of a pentagonal bipyramid. The coordination polyhedron of the anion is a distorted octahedron with a central uranium atom with five bromido ligands and one ethyl acetate molecule coordinating to it. A section of the crystal structure illustrating both ions is shown in Figure 1. The atomic distances between the uranium atom and the bromido ligands range from 2.7373(7) to 2.8223(7) Å in the cation and from 2.7460(7) to 2.7711(8) Å in the anion. This is comparable to distances in compounds like $[NEt_4]_2[UBr_4(t\text{-butylimido})_2]$.[34,55] The C−H···Br hydrogen bonds between the ethyl acetate and the bromido ligands range from 3.546(9) to 4.092(9) Å and are in good agreement with the literature.[40,55,56] Selected L−U−L (L = coordinating ligand atom) angles in the octahedral $[UBr_5(EtOAc)]^-$ anion range from 81.93(13) to 99.41(3)° and show a significant distortion of the coordination polyhedron. The pentagonal bipyramidal $[UBr_3(EtOAc)_4]^+$ cation is only slightly distorted with angles between 69.64(16) and 74.30(12)° (ideal 72°) for the equatorial ligands and between 87.19(13) and 92.95(2)° (ideal 90°) for the axial ligands. The closest U···U distances are between neighboring cations and anions with ca. 7.72 Å. This is slightly larger compared to the chloride above. As in the chloride, the cations are surrounded by six anions in the shape of quite distorted octahedra and vice versa with U···U distances in the range from ca. 7.72 to 9.97 Å. However, the distortions are less pronounced compared to the chloride. Therefore, the cations of the compound form a distorted cubic close packing with the anions residing in the vicinity of its octahedral voids. That is, the bromide compound is related to

https://doi.org/10.1021/acsomega.2c00175
ACS Omega 2022, 7, 11995−12003

Table 1. Selected Crystallographic Data and Details of the Structure Determinations of the Uranium(IV) Halide Ethyl Acetate Complexes

formula	$[UCl_3(EtOAc)_4][UCl_5(EtOAc)]$	$[UBr_3(EtOAc)_4][UBr_5(EtOAc)]$	$[UI_4(EtOAc)_3]$
molar mass/g·mol^{-1}	1200.18	1555.86	1009.94
space group (no.)	$P2_12_12_1$ (19)	$P12_1/n1$ (14)	$P2_1/c$ (14)
a/Å	15.1255(4)	15.7380(10)	15.085(3)
b/Å	15.4634(7)	17.5732(9)	11.753(2)
c/Å	17.4324(7)	16.2532(11)	14.176(3)
β/°	90	113.853(5)	93.93(3)
V/Å^3	4077.3(3)	4111.2(2)	2507.4(9)
Z	4	4	4
Pearson symbol	*o*P320 w. H atoms	*m*P320 w. H atoms	*m*P188 w. H atoms
ρ_{calcd}/g·cm^{-3}	1.955	2.514	2.675
μ/mm^{-1}	8.496	15.682	11.417
color	dark blue	dark green	dark red
crystal morphology	block	block	block
crystal size/mm^3	0.15 × 0.10 × 0.08	0.20 × 0.10 × 0.07	0.10 × 0.08 × 0.06
T/K	250(2)	100(2)	100(2)
λ/Å	0.71073 (Mo K_α)	0.71073 (Mo K_α)	0.71073 k
no. of reflections	42194	57562	36981
θ range/°	2.634−25.028	2.606−27.984	2.577−26.833
range of Miller indices	$-18 \le h \le 15$	$-20 \le h \le 20$	$-19 \le h \le 19$
	$-18 \le k \le 18$	$-23 \le k \le 23$	$-14 \le k \le 14$
	$-20 \le l \le 20$	$-21 \le l \le 19$	$-17 \le l \le 17$
absorption correction	numerical	numerical	numerical
T_{max}, T_{min}	0.2722, 0.3859	0.0738, 0.3021	0.1784, 0.5198
R_{int}, R_σ	0.0620, 0.0390	0.0415, 0.0866	0.0506, 0.1142
completeness of the data set	1.000	0.973	0.992
no. of unique reflections	7193	9651	5333
no. of parameters	429	371	214
no. of restrains	446	0	0
no. of constrains	0	0	0
S (all data)	1.002	1.036	1.013
$R(F)$ ($I \ge 2\sigma(I)$, all data)	0.0312, 0.0631	0.0360, 0.0525	0.0313, 0.0450
$wR(F^2)$ ($I \ge 2\sigma(I)$, all data)	0.0522, 0.0591	0.0776, 0.0839	0.0690, 0.0730
$\Delta\rho_{max}$, $\Delta\rho_{min}$/e·Å^{-3}	0.607, −0.650	1.523, −1.818	1.587, −0.732
flack x	0.393(10)	-	-

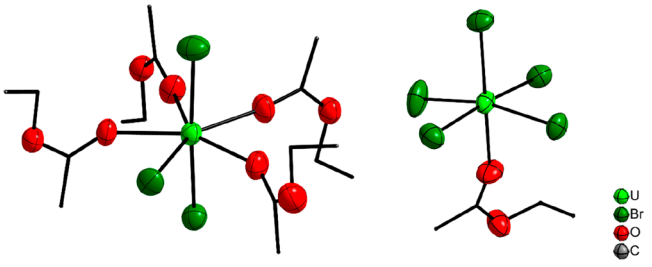

Figure 1. Sections of the crystal structures, the pentagonal bipyramidal $[UX_3(EtOAc)_4]^+$ cation (on the left), and the octahedron like $[UX_5(EtOAc)]^-$ anion (on the right) of $[UX_3(EtOAc)_4]$-$[UX_5(EtOAc)]$ with X = Cl and Br. The displacement ellipsoids are shown at the 70% probability level at 100 K. Hydrogen atoms are omitted, and carbon atoms are shown as a wire frame for clarity.

the NaCl structure type. For the chloride, too much distortion is present, preventing this structure relation.

We first thought that the orthorhombic chloride compound could represent a high-temperature polymorph structurally related to the low-temperature monoclinic bromide compound. As there is no direct group-subgroup relation between the respective space groups, a displacive phase transition can be ruled out, but a reconstructive phase transition could still be possible. Usually, higher symmetry is present in high-temperature phases, which is not the case here. The crystal structure of the bromide, monoclinic with space group $P12_1/n1$ at 100 K, shows a recognizable relation to the NaCl structure type, whereas the crystal structure of the chloride, orthorhombic with space group $P2_12_12_1$ at 250 K, does not.

Crystal Structure of the Iodide. The reaction of uranium(IV) iodide in ethyl acetate at room temperature leads to the formation of dark red crystals of $[UI_4(EtOAc)_3]$. The compound does not show self-ionization and crystallizes in the monoclinic crystal system $P2_1/c$, No. 14, with a = 15.085(3), b = 11.753(2), c = 14.176(3) Å, β = 93.93(3)°, V = 2507.4(9) Å^3, and Z = 4 at T = 100 K. Although the anions $[UI_5L]^-$ and $[UI_6]^{2-}$ are known, a formation of one of these was not observed by us at various temperatures (−35 to 70 °C).[37,41] The uranium atom is surrounded by the shape of a slightly distorted pentagonal bipyramid by four iodine and three oxygen atoms (Figure 2). The atomic distances between the U atom and the iodido ligands range from 2.9938(6) to 3.11525(8) Å and for the coordinating O atoms of the ethyl acetate ligands from 2.316(4) to 2.349(4) Å. These distances are in agreement with the literature.[57−59] The large iodido ligands next to the small O ligand atoms of the ethyl acetate molecules induce a distortion of the pentagonal bipyramidal

https://doi.org/10.1021/acsomega.2c00175
ACS Omega 2022, 7, 11995−12003

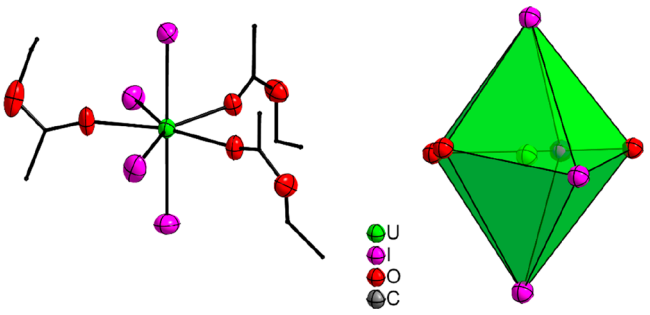

Figure 2. Left: Section of the crystal structure of $[UI_4(EtOAc)_3]$. The displacement ellipsoids are shown at the 70% probability level at 100 K. Hydrogen atoms are omitted, and carbon atoms are shown as a wire frame for clarity. Right: Polyhedron showing the distortion of the pentagonal bipyramid. Atoms are shown isotropic with arbitrary radii.

coordination sphere, with L−U−L (L = coordinating ligand atom) angles between 68.36(14) and 74.84(10)° (ideal 72°) for equatorial and between 87.95(11) and 94.49(10)° (ideal 90°) for axial ligands (Figure 2).

The packing of the molecules of the iodide, that is their U atoms, corresponds to the Mg structure type with the hexagonal close-packed layers parallel to the *bc* plane. The closest U···U distances are ca. 8.24 Å.

IR and Raman Spectroscopic Investigations. The ATR IR spectra of the three compounds (Figures S1−S3) were recorded at room temperature and are dominated by the vibration bands of the ethyl acetate ligands. The bands of the C−H stretching modes are observed around 2936 and 2983 cm^{-1} and for the C−O−C stretching modes at 1315 and 1034 cm^{-1}, which is in good agreement with noncoordinating ethyl acetate.[60] The C═O stretching modes of the chloride, the bromide, and the iodide reported here are observed at 1610, 1603, and 1601 cm^{-1}, respectively. The bathochromic shift of 131−140 cm^{-1}, compared to the free ester, is attributed to a significant weakening of the C═O bond. This is indicative for a strong interaction of the uranium atoms with the coordinating carbonyl oxygen atoms and is typical for carboxylic acid ester complexes of strongly Lewis acidic metals.[61] The uranium halide U−X (X = Cl, Br, I) stretching frequencies do not show intensities in the region accessible to our instrument from 4000 to 400 cm^{-1}.[62−64] Also, there is no hint toward characteristic bands of commonly observed impurities such as the uranyl cation UO_2^{2+} that would give rise to a band in the region from ∼911 to 960 cm^{-1}.[65]

The Raman spectra of the compounds (Figure S4) were also recorded at room temperature and are comparable to the Raman spectrum of free ethyl acetate.[66] An overview of the band assignment is given in Table 2, and other bands could not be assigned unambiguously.

NMR Spectroscopic Investigations. ^1H and ^{13}C NMR spectroscopy was used to investigate which species is present in the solutions of the title compounds. Therefore, crystals of the compounds were dissolved in CD_2Cl_2. The applicability of NMR spectroscopy for the analysis of uranium(IV) compounds is limited due to its paramagnetism. Due to coupling between nuclear and electron spins, the chemical shift becomes unpredictable, and the signals are broadened, sometimes to an extent that they are not observable.[68] The ^1H and ^{13}C NMR spectra of the title compounds show discrete signals for the two methyl groups, the methylene group, and the carbon nucleus of the carbonyl group, respectively. However, all signals are broadened and show significant paramagnetic shifts (Figure 3).

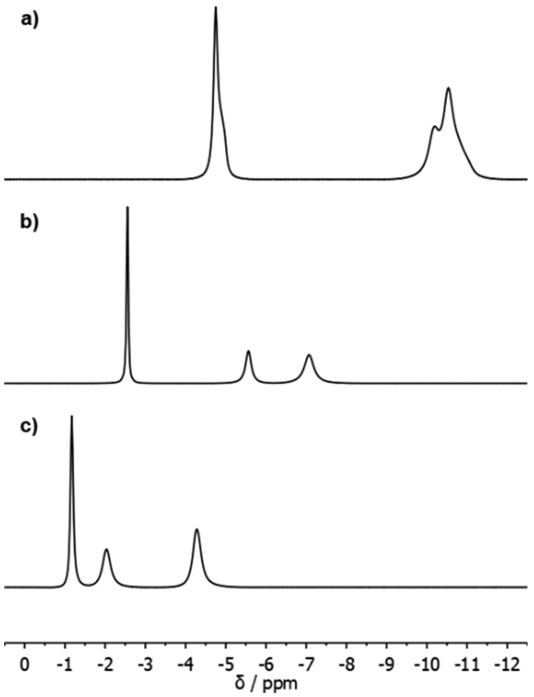

Figure 3. ^1H NMR spectra of (a) $[UCl_3(EtOAc)_4][UCl_5(EtOAc)]$, (b) $[UBr_3(EtOAc)_4][UBr_5(EtOAc)]$, and (c) $[UI_4(EtOAc)_3]$ in CD_2Cl_2.

All ^1H NMR signals are shifted upfield in comparison to noncoordinated ethyl acetate.[69] In the ^{13}C NMR spectra, only the signals of the methyl carbon nuclei are shifted upfield, while the signal of the methylene carbon nucleus is shifted upfield in the case of the chloride and bromide compounds and downfield in the iodide. Only in the chloride complex the signal of the carbonyl carbon nucleus is shifted upfield, whereas

Table 2. Selected Raman Bands and Assignment of the Three Title Compounds[66,67]

$[UCl_3(EtOAc)_4][UCl_5(EtOAc)]$	$[UBr_3(EtOAc)_4][UBr_5(EtOAc)]$	$[UI_4(EtOAc)_3]$	EtOAc	
390	391	389	381	δ(C−C), m
637	641	703	697	γ(CH_3COO), w
852	858	847	849	ν(C−C), w
1120	1125	1115	1117	ν(skeletal), m
1666	1659	1743	1738	ν(C═O), m
2881	2886	2878	2879	ν(CH), m
2936	2932	2937	2943	ν(CH), vs
2978	2977	2974	2974	ν(CH), s

https://doi.org/10.1021/acsomega.2c00175
ACS Omega 2022, 7, 11995−12003

Table 3. NMR Chemical Shifts of $[UCl_3(EtOAc)_4][UCl_5(EtOAc)]$, $[UBr_3(EtOAc)_4][UBr_5(EtOAc)]$, and $[UI_4(EtOAc)_3]$ and Respective Coordination Shifts of Ethyl Acetate in CD_2Cl_2

	CH_2CH_3				$C(O)CH_3$				CH_2CH_3				$C(O)$	
	^1H/ppm		^{13}C/ppm		^1H/ppm		^{13}C/ppm		^1H/ppm		^{13}C/ppm		^{13}C/ppm	
	δ	$\Delta\delta$	δ	$\Delta\delta$	δ	$\Delta\delta$	δ	$\Delta\delta$	δ	$\Delta\delta$	δ	$\Delta\delta$	δ	$\Delta\delta$
Cl	−4.75	−5.98	5.7	−8.7	−10.55	−12.55	5.2	−16.0	−10.17	−14.25	51.3	−9.3	154.9	−16.3
Br	−2.56	−3.79	8.4	−6.0	−7.07	−9.07	12.5	−8.7	−5.56	−9.64	58.2	−2.4	174.3	3.1
I	−1.17	−2.40	10.5	−3.9	−4.28	−6.28	20.0	−1.2	−2.03	−6.11	62.6	2.0	188.7	17.5

in the bromide and iodide these signals are shifted downfield (Table 3). The coordination shift increases from the iodide via the bromide to the chloride compound, which indicates increasing interaction between the uranium atoms and the ester ligands. This is in line with expectations due to the increasing electronegativity of the halides. This results in lower electron density at the metal center and increasing U−O bond strength from $[UI_4(EtOAc)_3]$ via $[UBr_3(EtOAc)_4][UBr_5(EtOAc)]$ to $[UCl_3(EtOAc)_4][UCl_5(EtOAc)]$ as is expected also from the Pearson concept of hard and soft Lewis acids and bases.

Even though some uncoordinated ethyl acetate was present in all NMR samples, only one signal set was observed. This indicates fast exchange between free and coordinated ester ligands on the NMR time scale, which results in an average signal. Therefore, also fast exchange between the EtOAc ligands of the $[UX_3(EtOAc)_4]^+$ and $[UX_5(EtOAc)]^-$ ions is expected, which would also lead to the observation of only one signal set. Since also neutral $[UX_4(EtOAc)_3]$ would give only one signal set in ^1H and ^{13}C NMR spectra and the paramagnetism of U(IV) leads to unpredictable chemical shifts, signals of $[UX_3(EtOAc)_4][UX_5(EtOAc)]$ and $[UX_4(EtOAc)_3]$ are indistinguishable in the NMR spectra. Thus, no conclusions may be drawn, whether self-ionization also occurs in solution.

Quantum Chemical Calculations. To clarify the self-ionization behavior, we studied the thermodynamics of reaction 1 for X = Cl, Br, and I with quantum chemical methods (DFT-PBE0/def2-TZVP, see the Experimental Section for the computational details).

$$2[UX_4(EtOAc)_3] \rightarrow [UX_3(EtOAc)_4][UX_5(EtOAc)] + EtOAc \quad (1)$$

The conductor-like screening model (COSMO) was used to simulate the influence of the EtOAc solvent (relative dielectric constant of 6).[70] We evaluated the reaction energies at 0 K and the reaction Gibbs free energies at 298 K (Table 4). The dissociation reaction 1 shows a positive reaction energy at 0 K for all halides with the iodide showing the least unfavorable one with +80 kJ/mol. Consideration of the Gibbs free energies does not change the picture. Overall, the reactions become thermodynamically more favorable but still show a positive ΔG, when moving from X = Cl to I, which is in contrast to the self-ionization observed within the crystal structures of the chloride and the bromide.

Table 4. Comparison of Reaction Energies at 0 K (ΔE) and Gibbs Free Energies at 298 K (ΔG^{298}) for the $[UX_4(EtOAc)_3]$ Species[a]

X	quantity	energy/kJ mol^{-1}
Cl	ΔE	105
	ΔG^{298}	84
Br	ΔE	111
	ΔG^{298}	64
I	ΔE	80
	ΔG^{298}	28

[a]Values obtained at the DFT-PBE0/def2-TZVP level of theory with COSMO solvent model (relative dielectric constant of EtOAc = 6).

We also tested the effect of an electrostatically ideal solvent with COSMO (dielectric constant of infinity). In this case, the reaction becomes thermodynamically slightly more favorable, but the trend remains contrary to the trend observed experimentally in the solid state: self-ionization is then thermodynamically favored for X = I and unfavored for X = Cl (Table S1 in Supporting Information).

In summary, the $[UX_4(EtOAc)_3]$ species are not expected to dissociate in EtOAc solution based on our DFT calculations. Of course, differently composed molecular species compared to $[UX_4(EtOAc)_3]$ could be present and involved in various equilibria upon crystallization of the compounds. However, we can confirm neither the existence nor the absence of such species from the NMR spectra.

CONCLUSION

The solid-state compounds $[UCl_3(EtOAc)_4][UCl_5(EtOAc)]$ and $[UBr_3(EtOAc)_4][UBr_5(EtOAc)]$ were obtained by self-ionization reactions of the respective uranium tetrahalide in the presence of the solvent and O-donor ligand ethyl acetate (EtOAc). UI_4 does not show the same reactivity under similar conditions, as a compound with the composition $[UI_4(EtOAc)_3]$ is obtained. The crystal structures of the chloride and bromide salts are not isotypic, despite both featuring isostructural complex ions with U atom coordination spheres of distorted pentagonal bipyramids for the cations and slightly distorted octahedra. As the chloride crystallizes orthorhombic, space group $P2_12_12_1$, and the bromide monoclinic, space group $P12_1/n1$, no direct group−subgroup relation is present excluding a displacive phase transition of an orthorhombic high-temperature to a monoclinic low-temperature phase. However, a reconstructive phase transition may of course be possible, or there simply is no structural relation between the two compounds. While the crystal structure of the bromide can be related to the NaCl structure type, the distortions within the chloride are so profound that no such relation became obvious. The packing of the molecules of the iodide corresponds to the Mg structure type.

In solution, only one signal set of coordinated ethyl acetate ligands can be observed with NMR spectroscopy. The spectra show that exchange on the NMR time scale occurs between the ethyl acetate ligands in solution. Thus, it remains unclear if self-ionization is also present in solution or if there is an effect of different solubilities and shifted equilibria of various

https://doi.org/10.1021/acsomega.2c00175
ACS Omega 2022, 7, 11995−12003

dissolved species due to the inset of crystallization of the compounds. IR and NMR spectra as well as quantum chemical calculations show the expected trend of decreasing bond strength and electronegativity from U−Cl to U−I.

Based on the DFT results, the $[UX_4(EtOAc)_3]$ species are not expected to dissociate in EtOAc solution under the studied conditions. So, the question why the chloride and bromide show autodissociation and the iodide does not remains currently unanswered.

EXPERIMENTAL SECTION

All work was carried out excluding moisture and air in an atmosphere of dried and purified argon (5.0, Praxair) using high vacuum glass lines and a glovebox (MBraun). Aluminum chloride and bromide (Merck, 98%/Alfa Aesar, 98%) were purified by sublimation in vacuo before use. Elemental iodine was sublimed in vacuo several times, the last time from phosphorus pentoxide. Aluminum powder (Fluka, purum >99%) was dried in vacuo at 250 °C. $UO_2(NO_3)_2{\cdot}6H_2O$ (Merck, p.a.) was used without further purification. Ethyl acetate was predried with P_4O_{10} and directly distilled onto the uranium halides.

Uranium compounds with natural U isotope distribution are radioactive, and appropriate measures for safe handling need to be taken.

The borosilicate glass vessels were flame-dried several times under a dynamic vacuum (10^{-3} mbar) before use. For the syntheses, glass ampules were used with a length of 16 cm, an outer diameter of 18 mm, and a wall thickness of 1.5 mm as described previously.[64,71] The top of the ampule carries an NS14.5 inner ground joint for filling of the educts and a constriction for easier flame sealing. The second constriction at one-third length of the ampule is used to allow for easier opening of the ampule after the reaction.

Synthesis of UO_2. Amounts of 12.8 g of $UO_2(NO_3)_2{\cdot}6H_2O$ (25.4 mmol) were decomposed to 7.13 g of U_3O_8 (8.47 mmol) by heating to 700 °C in air for 12 h inside an open silica test tube. The black product was powdered in air and reduced in a stream of hydrogen at 800 °C for 8 h to obtain 6.86 g (24.9 mmol, 98%) of phase-pure UO_2.

Synthesis of UCl_4. UCl_4 was synthesized according to the literature.[64] An ampule was charged with 1084 mg of UO_2 (4 mmol) and 1067 + 109 mg of $AlCl_3$ (8 mmol + transport agent) and flame-sealed under a vacuum (1×10^{-3} mbar). The starting materials were reacted at 250 °C for 12 h before the transport reaction was conducted with a source temperature of 350 °C and a sink temperature of 250 °C. An amount of 1428 mg (4.3 mmol, 94%) of green plate-shaped crystals of UCl_4 was obtained after 4 days.

Synthesis of UBr_4. UBr_4 was synthesized according to the literature.[64] An ampule was charged with 1088 mg of UO_2 (4 mmol) and 2150 + 65 mg of $AlBr_3$ (8 mmol + transport agent) and flame-sealed under a vacuum (1×10^{-3} mbar). The starting materials were reacted at 250 °C for 12 h before the transport reaction was conducted with a source temperature of 350 °C and a sink temperature of 230 °C. An amount of 1978 mg (4.3 mmol, 86%) of brown plate-shaped crystals of UBr_4 was obtained after 6 days.

Synthesis of UI_4. UI_4 was synthesized according to the literature.[64] An ampule was charged with 1003 mg of UO_2 (4 mmol), 3261 + 11 mg of AlI_3 (8 mmol + transport agent), and 238 mg of I_2 (2 bar I_2 at 350 °C) and flame-sealed under a vacuum (1×10^{-3} mbar). The starting materials were reacted at 250 °C for 12 h before the transport reaction was conducted with a source temperature of 350 °C and a sink temperature of 250 °C. An amount of 2714 mg (3.64 mmol, 91%) of needle-like black crystals of UI_4 was obtained after 5 days.

Synthesis of Trichlorido Tetra(ethyl acetate) Uranium(IV) Pentachloride (Ethyl Acetate) Uranate(IV) $[UCl_3(EtOAc)_4][UCl_5(EtOAc)]$. An amount of 25 mg (0.07 mmol) of UCl_4 was reacted with an excess of ethyl acetate (ca. 5 mL) in a Schlenk tube at room temperature. After the UCl_4 was dissolved completely, the excess of ethyl acetate was slowly removed under a vacuum to ca. 1 mL until crystallization was observed. Then the Schlenk tube was stored at 2 °C. Dark blueish crystals could be obtained after 7 days of storage. Yield was essentially quantitative.

^{1}H NMR (500 MHz, CD_2Cl_2): δ = −10.55 (bs, 3H, C(O)CH_3), −10.17 (bs, 2H, CH_2CH$_3$), −4.75 (bs, 3H, CH$_2$CH_3). ^{13}C NMR (126 MHz, CD_2Cl_2): δ = 5.2 (C(O)CH_3), 5.7 (CH$_2$CH_3), 51.3 (CH_2CH$_3$), 154.9 (C(O)).

Synthesis of Tribromido Tetra(ethyl acetate) Uranium(IV) Pentabromido (Ethyl Acetate) Uranate(IV) $[UBr_3(EtOAc)_4][UBr_5(EtOAc)]$. An amount of 25 mg (0.04 mmol) of UBr_4 was reacted with an excess of ethyl acetate (ca. 5 mL) in a Schlenk tube at room temperature. After the UBr_4 was dissolved completely, the excess of ethyl acetate was slowly removed under a vacuum to ca. 1 mL until crystallization was observed. Then the Schlenk tube was stored at 2 °C. Dark brown crystals could be obtained after 7 days of storage. Yield was essentially quantitative.

^{1}H NMR (500 MHz, CD_2Cl_2): δ = −7.07 (bs, 3H, C(O)CH_3), −5.56 (bs, 2H, CH_2CH$_3$), −2.56 (bs, 3H, CH$_2$CH_3). ^{13}C NMR (126 MHz, CD_2Cl_2): δ = 8.4 (CH$_2$CH_3), 12.5 (C(O)CH_3), 58.2 (CH_2CH$_3$), 174.3 (C(O)).

Synthesis of Tri(ethyl acetate) Tetraiodido Uranium-(IV) $[UI_4(EtOAc)_3]$. An amount of 40 mg (0.05 mmol) of UI_4 was reacted with an excess of ethyl acetate (ca. 5 mL) in a Schlenk tube at room temperature. After the UI_4 was dissolved completely, the excess of ethyl acetate was slowly removed under a vacuum to ca. 1 mL until crystallization was observed. Then the Schlenk tube was stored at 2 °C. Dark red crystals could be obtained after 5 days of storage. Yield was essentially quantitative.

^{1}H NMR (500 MHz, CD_2Cl_2): δ = −4.28 (bs, 3H, C(O)CH_3), −2.03 (bs, 2H, CH_2CH$_3$), −1.17 (bs, 3H, CH$_2$CH_3). ^{13}C NMR (126 MHz, CD_2Cl_2): δ = 10.5 (CH$_2$CH_3), 20.0 (C(O)CH_3), 62.6 (CH_2CH$_3$), 188.7 (C(O)).

Raman Spectroscopy. Raman spectra were recorded with a confocal raman microscope S+I MonoVista CRS+, using the 532 nm excitation line of an integrated diode laser (resolution <1 cm^{-1}; range 50−9000 cm^{-1}). A sample of the compound was located inside a 10 mm borosilicate glass Schlenk tube, which was flame-dried several times under vacuum before use. The spectra were processed with the OriginPro 2017 software package.[72]

IR Spectroscopy. The IR spectra were recorded on a Bruker alpha FT-IR spectrometer using the ATR Diamond module with a resolution of 4 cm^{-1}. The spectrometer was located inside a glovebox (MBraun) under an argon atmosphere. The spectra were processed with the OPUS software package.[73]

NMR Spectroscopy. ^{1}H and ^{13}C spectra were recorded on a Bruker Avance III 500 spectrometer equipped with a Prodigy Cryo-Probe. ^{1}H NMR (500 MHz) and ^{13}C NMR (126 MHz) chemical shifts are given relative to the solvent signal for

https://doi.org/10.1021/acsomega.2c00175
ACS Omega 2022, 7, 11995−12003

CD_2Cl_2 (5.32 and 54.0 ppm). NMR spectra were processed with the MestReNova software.[74]

Single-Crystal X-ray Diffraction. Single crystals of the compounds described above were selected at room temperature under predried perfluorinated oil and mounted using a MiTeGen loop. Intensity data of a suitable crystal were recorded with an IPDS 2T diffractometer (Stoe & Cie). The diffractometer was operated with Mo−K_α radiation (0.71073 Å, graphite monochromator) and equipped with an image plate detector. Evaluation, integration, and reduction of the diffraction data were carried out using the X-Area software suite.[75] Numerical absorption corrections were applied with the modules X-Shape and X-Red32 of the X-Area software suite. The structures were solved with dual-space methods (SHELXT-2018/2) and refined against F^2 (SHELXL-2018/3).[76,77] All atoms were refined with anisotropic displacement parameters, and H atom isotropic and riding models were adequate. Disorder was modeled using DSR.[78] Cif files were deposited with the CCDC (https://www.ccdc.cam.ac.uk/), depository numbers: 2124219−2124221 (X = I, Cl, Br).

Quantum chemical calculations. All calculations were carried out with the TURBOMOLE[79,80] program suite using the PBE0[81,82] hybrid density functional method (DFT-PBE0). Karlsruhe def2-TZVP[83] basis sets were applied for hydrogen, carbon, oxygen, chlorine, and bromine. For uranium and iodine, scalar relativistic effects were taken into account by using 60-electron effective core potentials,[84−86] together with respective def-TZVP and def2-TZVP valence basis sets.[87] Multipole-accelerated resolution-of-the-identity approximation (MA-RIJ) was used to speed up the DFT calculations,[88−90] and the m4 integration grid was used for the numerical integration of the exchange-correlation part. The conductor-like screening model (COSMO) was applied in all calculations to describe an ethyl acetate solvent field.[91] The geometries of the complexes were fully optimized within the constraints of their point group symmetries. Numerical harmonic frequency calculations were performed to check if the optimized structures are true local minima on the potential energy surface. The Cartesian coordinates of the optimized structures are available in the Supporting Information. The thermal contributions to the free enthalpy were obtained within the harmonic oscillator rigid rotor model at room temperature, using the *freeh* module. The harmonic frequencies were not scaled when evaluating the thermal contributions.

■ ASSOCIATED CONTENT

Supporting Information

The Supporting Information is available free of charge at https://pubs.acs.org/doi/10.1021/acsomega.2c00175.

Recorded IR, Raman, and NMR spectra as well as the technical details of the quantum chemical calculations (PDF)

CIF file for UBr_4_EtOAc (CIF)

CIF file for UCl_4_EtOAc (CIF)

CIF file for UI_4_EtOAc (CIF)

■ AUTHOR INFORMATION

Corresponding Author

Florian Kraus − *Philipps-Universität Marburg, Fachbereich Chemie, Marburg, Hessen 35032, Germany;* orcid.org/0000-0003-4368-8418; Email: f.kraus@uni-marburg.de

Authors

H. Lars Deubner − *Philipps-Universität Marburg, Fachbereich Chemie, Marburg, Hessen 35032, Germany*

Tim Graubner − *Philipps-Universität Marburg, Fachbereich Chemie, Marburg, Hessen 35032, Germany*

Magnus R. Buchner − *Philipps-Universität Marburg, Fachbereich Chemie, Marburg, Hessen 35032, Germany*

Florian Weigend − *Philipps-Universität Marburg, Fachbereich Chemie, Marburg, Hessen 35032, Germany;* orcid.org/0000-0001-5060-1689

Sergei I. Ivlev − *Philipps-Universität Marburg, Fachbereich Chemie, Marburg, Hessen 35032, Germany;* orcid.org/0000-0003-4871-825X

Antti J. Karttunen − *Aalto University, Department of Chemistry and Materials Science, Aalto 00076, Finland*

Complete contact information is available at: https://pubs.acs.org/10.1021/acsomega.2c00175

Notes

The authors declare no competing financial interest.

■ ACKNOWLEDGMENTS

We thank the Deutsche Forschungsgemeinschaft for funding. T.G. thanks the HPC-EUROPA3 (INFRAIA-2016-1-730897) for a travel grant and the computing resources provided by CSC, the Finnish IT Center for Science.

■ REFERENCES

(1) McLuckey, S. A.; Glish, G. L.; Asano, K. G.; Van Berkel, G. J. Self Chemical Ionization in an Ion Trap Mass Spectrometer. *Anal. Chem.* **1988**, *60* (20), 2312−2314.

(2) Pitzer, K. S. Self-Ionization of Water at High Temperature and the Thermodynamic Properties of the Ions. *J. Phys. Chem.* **1982**, *86* (24), 4704−4708.

(3) Christe, K. O.; Schack, C. J. Structure of Complexes between Bromine Trifluoride and Lewis Acids. *Inorg. Chem.* **1970**, *9* (10), 2296−2299.

(4) Christe, K. O.; Schack, C. J. The Tetrafluorobromate(III) Anion, BrF4-. *Inorg. Chem.* **1970**, *9* (8), 1852−1858.

(5) Finch, A.; Fitch, A. N.; Gates, P. N. Crystal and Molecular Structure of a Metastable Modification of Phosphorus Pentachloride. *J. Chem. Soc., Chem. Commun.* **1993**, No. 11, 957.

(6) Kamata, K.; Suzuki, A.; Nakai, Y.; Nakazawa, H. Catalytic Hydrosilylation of Alkenes by Iron Complexes Containing Terpyridine Derivatives as Ancillary Ligands. *Organometallics* **2012**, *31* (10), 3825−3828.

(7) Jander, G. *Die Chemie in wasserähnlichen Lösungsmitteln: Die Grundlagen des chemischen und physikalisch-chemischen Verhaltens der Stoffe in einigen nicht-wässrigen, aber wasserähnlichen Solventien*; Springer: Berlin, Heidelberg, 1949.

(8) Jander, J.; Lafrenz, C. *Chemische Taschenbücher 3 - Wasserähnliche Lösungsmittel*; Foerst, W., Grünewald, H., Eds.; Verlag Chemie: Weinheim, 1968.

(9) Doetsch, V.; Jander, J.; Engelhardt, U.; Lafrenz, C.; Fischer, J.; Nagel, H.; Renz, W.; Türk, G.; von Volkmann, T.; Weber, G. *Chemistry in Anhydrous Liquid Ammonia - Part 1 - Anorganische Und Allgemeine Chemie in Flüssigem Ammoniak*; Jander, G., Addison, C. C., Spandau, H., Series Eds.; Chemistry in Nonaqueous Ionizing Solvents; Friedr. Vieweg & Sohn: Braunschweig, 1966; Vol. *1*.

(10) Glemser, O. Halogen Chemistry. Von V. Gutmann. Academic Press, London-New York 1967. Band 1. 1. Aufl., XIII, 473 S., mehrere Abb. u. Tba., geb. $ 21.00/£ 6. *Angew. Chem.* **1968**, *80* (20), 856−856.

(11) Wilson, W. W.; Christe, K. O. Dinitrogen Pentoxide. New Synthesis and Laser Raman Spectrum. *Inorg. Chem.* **1987**, *26* (10), 1631−1633.

(12) Pavia, A. C.; Pascal, J. L.; Potier, A. *C. R. Acad. Sci. C Chim.* **1971**, *272*, 1495−1498.
(13) Powell, H. M.; Clark, D.; Wells, A. F. Crystal Structure of Phosphorus Pentachloride. *Nature* **1940**, *145* (3665), 149−149.
(14) Gabes, W.; Olie, K. Refinement of the Crystal Structure of Phosphorus Pentabromide, PBr5. *Acta Crystallogr., Sect. B: Struct. Crystallogr. Cryst. Chem.* **1970**, *26* (4), 443−444.
(15) Meinert, H.; Gross, U. Über die Eigenionisation der Halogenfluoride. *J. Fluorine Chem.* **1973**, *2* (4), 381−386.
(16) Grant, D. J.; Matus, M. H.; Switzer, J. R.; Dixon, D. A.; Francisco, J. S.; Christe, K. O. Bond Dissociation Energies in Second-Row Compounds. *J. Phys. Chem. A* **2008**, *112* (14), 3145−3156.
(17) Holleman, A. F.; Wiberg, E.; Wiberg, N. *Lehrbuch Der Anorganischen Chemie*, 102nd ed.; Walter de Gruyter: Berlin, 2007.
(18) Swidan, A.; Onge, P. B. J.; Binder, J. F.; Suter, R.; Burford, N.; Macdonald, C. L. B. 2,6-Bis(Benzimidazol-2-Yl)Pyridine Complexes of Group 14 Elements. *Dalton Trans.* **2019**, *48* (22), 7835−7843.
(19) Jurca, T.; Hiscock, L. K.; Korobkov, I.; Rowley, C. N.; Richeson, D. S. The Tipping Point of the Inert Pair Effect: Experimental and Computational Comparison of In(I) and Sn(II) Bis(Imino)Pyridine Complexes. *Dalton Trans.* **2014**, *43* (2), 690−697.
(20) Magdzinski, E.; Gobbo, P.; Workentin, M. S.; Ragogna, P. J. A Novel Diiminopyridine Ligand Containing Redox Active Co(III) Mixed Sandwich Complexes. *Inorg. Chem.* **2013**, *52* (19), 11311−11319.
(21) Decken, A.; Jenkins, H. D. B.; Knapp, C.; Nikiforov, G. B.; Passmore, J.; Rautiainen, J. M. The Autoionization of [TiF4] by Cation Complexation with [15]Crown-5 To Give [TiF2([15]Crown-5)][Ti4F18] Containing the Tetrahedral [Ti4F18]2− Ion. *Angew. Chem., Int. Ed.* **2005**, *44* (48), 7958−7961.
(22) Ališ, B.; Štefančič, A.; Tavčar, G. Small Molecule Activation: SbF_3 Auto-Ionization Supported by Transfer and Mesoionic NHC Rearrangement. *Dalton Trans.* **2017**, *46* (10), 3338−3346.
(23) Bourosh, P.; Bologa, O.; Simonov, Y.; Gerbeleu, N.; Lipkowski, J.; Gdaniec, M. Synthesis and Structure of Products of Interaction of H[AuCl4] with H2DMG and Pyridine. *Inorg. Chim. Acta* **2007**, *360* (10), 3250−3254.
(24) Jura, M.; Levason, W.; Ratnani, R.; Reid, G.; Webster, M. Six- and Eight-Coordinate Thio- and Seleno-Ether Complexes of NbF_5 and Some Comparisons with NbCl5 and NbBr5 Adducts. *Dalton Trans.* **2010**, *39* (3), 883−891.
(25) Marchetti, F.; Pampaloni, G. Interaction of Niobium and Tantalum Pentahalides with O-Donors: Coordination Chemistry and Activation Reactions. *Chem. Commun.* **2012**, *48* (5), 635−653.
(26) Levason, W.; Reid, G.; Zhang, W. Six-Coordinate NbF5 and TaF5 Complexes with Tertiary Mono-Phosphine and -Arsine Ligands. *J. Fluorine Chem.* **2015**, *172*, 62−67.
(27) Haiges, R.; Deokar, P.; Christe, K. O. Coordination Adducts of Niobium(V) and Tantalum(V) Azide $M(N_3)_5$ (M = Nb, Ta) with Nitrogen Donor Ligands and Their Self-Ionization. *Angew. Chem., Int. Ed.* **2014**, *53* (21), 5431−5434.
(28) Müller, M.; Buchner, M. R. Solution Behavior of Beryllium Halides in Dimethylformamide. *Inorg. Chem.* **2019**, *58* (19), 13276−13284.
(29) Müller, M.; Buchner, M. R. Diphenylberyllium Reinvestigated: Structure, Properties, and Reactivity of BePh2, [(12-Crown-4)-BePh]+, and [BePh3]−. *Chem. Eur. J.* **2020**, *26* (44), 9915−9922.
(30) Alvey, P. J.; Bagnall, K. W.; Brown, D.; Edwards, J. Sulfoxide Complexes of Actinoid Tetrahalides. *J. Chem. Soc., Dalton Trans.* **1973**, No. 21, 2308−2314.
(31) Bombieri, G.; Bagnall, K. W. X-Ray Crystal and Molecular Structure of UCl4,3Me2SO: Dichlorohexakis-(Dimethyl Sulfoxide) Uranium Hexachlorouranate [UCl2(Me2SO)6][UCl6]. *J. Chem. Soc., Chem. Commun.* **1975**, No. 6, 188−189.
(32) de Villardi, G. C.; Charpin, P.; Costes, R.-M.; Folcher, G.; Plurien, P.; Rigny, P.; de Rango, C. Uranium(IV)-Crown-Ether Complexes and Cryptates. 1H Nuclear Magnetic Resonance Study, and X-Ray Crystal and Molecular Structure of Tetrachloro-(2,5,8,15,18,21-Hexaoxatricyclo[20.4.0.09,14]Hexacosane)Uranium-(IV). *J. Chem. Soc., Chem. Commun.* **1978**, No. 3, 90.
(33) Bagnall, K. W.; Beddoes, R. L.; Mills, O. S.; Xing-fu, L. NN-Dimethyl- and NN-Diethyl-Propionamide Complexes of Uranium Tetrachloride; Crystal Structure of Trichlorotetrakis(NN-Diethylpropion- Amide)Uranium(IV) Pentachloro(NN-Diethylpropionamide)-Uranate(IV), [UCl3(EtCONEt2)4]+[UCl5(EtCONEt2)]? *J. Chem. Soc., Dalton Trans.* **1982**, No. 7, 1361.
(34) Beeckman, W.; Goffart, J.; Rebizant, J.; Spirlet, M. R. The First Cationic Indenyl-f-Metal Complexes with Pentagonal Bipyramidal Geometry. Crystal Structures of [C9H7UBr2(CH3CN)4]+2 [UBr6]2− and [{C9H7UBr(CH3CN)4}2O]2+ [UBr62−. *J. Organomet. Chem.* **1986**, *307* (1), 23−37.
(35) Charpin, P.; Nierlich, M.; Vigner, D.; Marquet-Ellis, H. N,N-Dimethylformamide−Uranium Tetrachloride Complex: Structure of Trichloropentakis(N,N-Dimethylformamide)Uranium(IV) Hexachlorouranate(IV). *Acta Crystallogr., Sect. C: Cryst. Struct. Commun.* **1988**, *44* (2), 257−259.
(36) Berthet, J.-C.; Thuery, P.; Ephritikhine, M. New Efficient Synthesis of $[UI_4(MeCN)_4]$. X-Ray Crystal Structures of $[UI_2(MeCN)_7][UI_6]$, $[UI_4(Py)_3]$, and [U(Dmf)9]I4. *Inorg. Chem.* **2005**, *44*, 1142−1146.
(37) Enriquez, A. E.; Scott, B. L.; Neu, M. P. Uranium(III)/(IV) Nitrile Adducts Including UI4(N⋮CPh)4, a Synthetically Useful Uranium(IV) Complex. *Inorg. Chem.* **2005**, *44* (21), 7403−7413.
(38) Wahu, S.; Berthet, J. C.; Thuery, P.; Bresson, C. *CCDC 1057445: Experimental Crystal Structure Determination* **2015**, DOI: 10.5517/cc14hc44.
(39) Wahu, S.; Berthet, J. C.; Thuery, P.; Bresson, C. *CCDC 1057446: Experimental Crystal Structure Determination* **2015**, DOI: 10.5517/cc14hc55.
(40) Siffredi, G.; Berthet, J. C.; Thuery, P.; Ephritikhine, M. CCDC 958359: Experimental Crystal Structure Determination, 2014. DOI: 10.5517/cc1157t8.
(41) Schnaars, D. D.; Wu, G.; Hayton, T. W. Reactivity of UI4(OEt2)2 with Phenols: Probing the Chemistry of the U−I Bond. *Dalton Trans.* **2009**, No. 19, 3681.
(42) Feinstein, H. I. *TEI-555 The Determination of Uranium in Ores: Separation by Ethyl Acetate Extraction and Spectrophotometric Determination by the Thiocyanate Method in Acetone-Water Medium*; TEI-555; U. S. Department of the Interior: Washington, D. C., 1955. DOI: 10.3133/tei555.
(43) Ward, F. N.; Price, V. Analytical Methodology for Uranium Exploration — Retrospective and Prospective. *J. Geochem. Explor.* **1980**, *13* (2−3), 97−113.
(44) Milner, G. W. C.; Wilson, J. D.; Barnett, G. A.; Smales, A. A. The Determination of Uranium in Sea Water by Pulse Polarography. *J. Electroanal. Chem.* **1961**, *2* (1), 25−38.
(45) Brunzie, G. F.; Johnson, T. R.; Steunenberg, R. K. Selective Dissolution of Uranium from Uranium-Uranium Oxide Mixtures by Bromine-Ethyl Acetate. *Anal. Chem.* **1961**, *33* (8), 1005−1006.
(46) Lai, T.-T.; Lin, H.-T. Solvent Extraction of Uranyl Thiocyanate Complex. I. *J. Chin. Chem. Soc. (Weinheim, Ger.)* **1961**, *8* (4), 327−333.
(47) Wassef, M. A.; Hegazi, W. S.; Ali, S. A. Coordination Compounds of Uranium(VI) with Lewis Bases. *J. Coord. Chem.* **1983**, *12* (2), 97−103.
(48) du Preez, J. G. H.; Rohwer, H. E.; van Brecht, B. J. A. M.; Zeelie, B.; Casellato, U.; Graziani, R. The Chemistry of Uranium. Part 41. Complexes of Uranium Tetrahalide, with Emphasis on Iodide, and Triphenylphosphine Oxide, Tris(Dimethylamino)Phosphine Oxide or Tris(Pyrrolidinyl)Phosphine Oxide. Crystal Structure of Tetrabromobis[Tris(Pyrrolidinyl)Phosphine Oxide]Uranium(IV). *Inorg. Chim. Acta* **1991**, *189* (1), 67−75.
(49) Al-Daher, A. G. M.; Bagnall, K. W. Some New Complexes of Thorium and Uranium Tetrabromides with Phosphine Oxides. *J. Less-Common Met.* **1986**, *116* (2), 359−367.

https://doi.org/10.1021/acsomega.2c00175
ACS Omega 2022, 7, 11995−12003

(50) Deshpande, S. G.; Jain, S. C. Mixed Ligand Complexes of Uranium. *Indian J. Chem., Sect. A: Inorg., Bio-inorg., Phys., Theor. Anal. Chem.* **1988**, *27A*, 552−554.
(51) Zhai, X.-S.; Zheng, Y.-Q.; Lin, J.-L.; Xu, W. Four New Dinuclear Uranyl Complexes Based on p - and m -Toluic Acid: Syntheses, Structures, Luminescent and Photocatalytic Properties. *Inorg. Chim. Acta* **2014**, *423*, 1−10.
(52) Klepov, V. V.; Serezhkina, L. B.; Grigor'ev, M. S.; Ignatenko, E. O.; Serezhkin, V. N. Uranyl Methacrylate Complexes with Carbamide and Methylcarbamide: Synthesis and Structure. *Russ. J. Inorg. Chem.* **2018**, *63* (8), 1019−1025.
(53) Nassimbeni, L. R.; Orpen, A. G.; Pauptit, R.; Rodgers, A. L.; Haigh, J. M. The Structure of Aliphatic Amine Adducts of Uranyl Acetylacetonate. II. Dioxobis(2,4-Pentanedionato)Mono(2-N,N-Dimethylaminopentan-4-One)Uranium(IV). *Acta Crystallogr., Sect. B: Struct. Crystallogr. Cryst. Chem.* **1977**, *33* (4), 959−962.
(54) Kim, J.-Y.; Norquist, A. J.; O'Hare, D. Variable Dimensionality in the $UO_2(CH_3CO_2)_2 \cdot 2H_2O$/HF/Isonicotinic Acid System: Synthesis and Structures of Zero-, One-, and Two-Dimensional Uranium Isonicotinates. *Chem. Mater.* **2003**, *15* (10), 1970−1975.
(55) Spencer, L. P.; Yang, P.; Minasian, S. G.; Jilek, R. E.; Batista, E. R.; Boland, K. S.; Boncella, J. M.; Conradson, S. D.; Clark, D. L.; Hayton, T. W.; Kozimor, S. A.; Martin, R. L.; MacInnes, M. M.; Olson, A. C.; Scott, B. L.; Shuh, D. K.; Wilkerson, M. P. Tetrahalide Complexes of the $[U(NR)_2]^{2+}$ Ion: Synthesis, Theory, and Chlorine K-Edge X-Ray Absorption Spectroscopy. *J. Am. Chem. Soc.* **2013**, *135* (6), 2279−2290.
(56) Andrews, M. B.; Cahill, C. L. Utilizing Hydrogen Bonds and Halogen−Halogen Interactions in the Design of Uranyl Hybrid Materials. *Dalton Trans.* **2012**, *41* (14), 3911−3914.
(57) Berthet, J.-C.; Nierlich, M.; Ephritikhine, M. A Comparison of Analogous 4f- and 5f-Element Compounds: Syntheses and Crystal Structures of Triphenylphosphine Oxide Complexes of Lanthanide(III) and Uranium(III) Triflates and Iodides [MX2(OPPh3)4][X] (X = OTf and M = Ce or U; X = I and M = Nd, Ce, La, U). *Polyhedron* **2003**, *22* (27), 3475−3482.
(58) Carmichael, C. D.; Jones, N. A.; Arnold, P. L. Low-Valent Uranium Iodides: Straightforward Solution Syntheses of UI_3 and UI_4 Etherates. *Inorg. Chem.* **2008**, *47* (19), 8577−8579.
(59) Heinemann, F. W.; Löffler, S.; Meyer, K. CCDC 1876221: Experimental Crystal Structure Determination, 2018. DOI: 10.5517/ccdc.csd.cc20zc8n.
(60) Oki, M.; Nakanishi, H. Conformations of the Ester Group. *Bull. Chem. Soc. Jpn.* **1970**, *43* (8), 2558−2566.
(61) Scheibe, B.; Buchner, M. R. Carboxylic Acid Ester Adducts of Beryllium Chloride and Their Role in the Synthesis of Beryllium Nitrates. *Eur. J. Inorg. Chem.* **2018**, *2018* (20−21), 2300−2308.
(62) Bohres, E. W.; Krasser, W.; Schenk, H.-J.; Schwochau, K. Schwingunsspektren und Kraftkonstanten der Actinid(IV)chloride ThCl4, PaCl4, UCl4 und NpCl4. *J. Inorg. Nucl. Chem.* **1974**, *36* (4), 809−813.
(63) Kovba, V. M.; Chikh, I. V. IR Spectra of Vapors over UF4, UCl4, UBr4, and in the UCl4?Cl2 System. *J. Struct. Chem.* **1983**, *24* (2), 326−327.
(64) Rudel, S. S.; Kraus, F. Facile Syntheses of Pure Uranium Halides: UCl_4, UBr_4 and UI_4. *Dalton Trans.* **2017**, *46* (18), 5835−5842.
(65) Bullock, J. I. Raman and Infrared Spectroscopic Studies of the Uranyl Ion: The Symmetric Stretching Frequency, Force Constants, and Bond Lengths. *J. Chem. Soc. A* **1969**, 781.
(66) https://Sdbs.Db.Aist.Go.Jp/Sdbs/Cgi-Bin/Landingpage?Sdbsno=889 National Institute of Advanced Industrial Science and Technology, 2019 (accessed July 21, 2021).
(67) Neelakantan, P. Raman Spectra of Liquid Mixtures (Cyclohexanol and Ethyl Acetate). *Proc. Indian Acad. Sci.* **1963**, *57* (6), 330−336.
(68) Schwarzhans, K. E. NMR-Spektroskopie an Paramagnetischen Komplexverbindungen. *Angew. Chem.* **1970**, *82* (24), 975−982.
(69) Fulmer, G. R.; Miller, A. J. M.; Sherden, N. H.; Gottlieb, H. E.; Nudelman, A.; Stoltz, B. M.; Bercaw, J. E.; Goldberg, K. I. NMR Chemical Shifts of Trace Impurities: Common Laboratory Solvents, Organics, and Gases in Deuterated Solvents Relevant to the Organometallic Chemist. *Organometallics* **2010**, *29* (9), 2176−2179.
(70) Nilles, G. P.; Schuetz, R. D. Selected Properties of Selected Solvents. *J. Chem. Educ.* **1973**, *50* (4), 267.
(71) Deubner, H. L.; Rudel, S. S.; Kraus, F. A Simple Access to Pure Thorium(IV) Halides ($ThCl_4$, $ThBr_4$, and ThI_4). *Z. Anorg. Allg. Chem.* **2017**, *643*, 2005−2010.
(72) OriginPro 2017; OriginLAb Corporation, 2017.
(73) *OPUS V7.2*; Bruker Optik GmbH: Ettlingen, Germany, 2012.
(74) *MestReNova*; Mestrelab Research S.L.: Santiago de Compostela, 2011.
(75) X-Area; STOE & Cie GmbH: Darmstadt, Germany, 2018.
(76) Sheldrick, G. M. SHELXT − Integrated Space-Group and Crystal-Structure Determination. *Acta Crystallogr., Sect. A: Found. Adv.* **2015**, *71* (1), 3−8.
(77) Sheldrick, G. M. Crystal Structure Refinement with *SHELXL*. *Acta Crystallogr., Sect. C: Struct. Chem.* **2015**, *71* (1), 3−8.
(78) Kratzert, D.; Krossing, I. Recent Improvements in *DSR*. *J. Appl. Crystallogr.* **2018**, *51* (3), 928−934.
(79) *TURBOMOLE V7.5, a Development of University of Karlsruhe and Forschungszentrum Karlsruhe GmbH, 1989−2007, TURBOMOLE GmbH, since 2007*; 2020.
(80) Ahlrichs, R.; Bär, M.; Häser, M.; Horn, H.; Kölmel, C. Electronic Structure Calculations on Workstation Computers: The Program System Turbomole. *Chem. Phys. Lett.* **1989**, *162* (3), 165−169.
(81) Adamo, C.; Barone, V. Toward Reliable Density Functional Methods without Adjustable Parameters: The PBE0Model. *J. Chem. Phys.* **1999**, *110* (13), 6158−6170.
(82) Perdew, J. P.; Burke, K.; Ernzerhof, M. Generalized Gradient Approximation Made Simple. *Phys. Rev. Lett.* **1996**, *77* (18), 3865−3868.
(83) Weigend, F.; Ahlrichs, R. Balanced Basis Sets of Split Valence, Triple Zeta Valence and Quadruple Zeta Valence Quality for H to Rn: Design and Assessment of Accuracy. *Phys. Chem. Chem. Phys.* **2005**, *7* (18), 3297−3305.
(84) Peterson, K. A.; Figgen, D.; Goll, E.; Stoll, H.; Dolg, M. Systematically Convergent Basis Sets with Relativistic Pseudopotentials. II. Small-Core Pseudopotentials and Correlation Consistent Basis Sets for the Post- *d* Group 16−18 Elements. *J. Chem. Phys.* **2003**, *119* (21), 11113−11123.
(85) Küchle, W.; Dolg, M.; Stoll, H.; Preuss, H. Energy-adjusted Pseudopotentials for the Actinides. Parameter Sets and Test Calculations for Thorium and Thorium Monoxide. *J. Chem. Phys.* **1994**, *100* (10), 7535−7542.
(86) Cao, X.; Dolg, M.; Stoll, H. Valence Basis Sets for Relativistic Energy-Consistent Small-Core Actinide Pseudopotentials. *J. Chem. Phys.* **2003**, *118* (2), 487−496.
(87) Cao, X.; Dolg, M. Segmented Contraction Scheme for Small-Core Actinide Pseudopotential Basis Sets. *J. Mol. Struct.: THEOCHEM* **2004**, *673* (1), 203−209.
(88) Weigend, F. A Fully Direct RI-HF Algorithm: Implementation, Optimised Auxiliary Basis Sets, Demonstration of Accuracy and Efficiency. *Phys. Chem. Chem. Phys.* **2002**, *4* (18), 4285−4291.
(89) Eichkorn, K.; Treutler, O.; Öhm, H.; Häser, M.; Ahlrichs, R. Auxiliary Basis Sets to Approximate Coulomb Potentials. *Chem. Phys. Lett.* **1995**, *240* (4), 283−290.
(90) Sierka, M.; Hogekamp, A.; Ahlrichs, R. Fast Evaluation of the Coulomb Potential for Electron Densities Using Multipole Accelerated Resolution of Identity Approximation. *J. Chem. Phys.* **2003**, *118* (20), 9136−9148.
(91) Klamt, A.; Schuurmann, G. COSMO: A New Approach to Dielectric Screening in Solvents with Explicit Expressions for the Screening Energy and Its Gradient. *J. Chem. Soc., Perkin Trans. 2* **1993**, No. 5, 799−805.

https://doi.org/10.1021/acsomega.2c00175
ACS Omega 2022, 7, 11995−12003